energies

MDPI

*Article*

# Design and Experimental Investigation of a Self-Powered Fan Based on a Thermoelectric System

**Huaibin Gao [1,*], Xiaojiang Liu [1], Chuanwei Zhang [1], Yu Ma [1], Hongjun Li [2] and Guanghong Huang [2]**

[1] School of Mechanical Engineering, Xi'an University of Science and Technology, Xi'an 710054, China
[2] Special Equipment Research Institute of Xi'an, Xi'an 710032, China
* Correspondence: gaohuaibin@xust.edu.cn

**Abstract:** Providing electricity for isolated areas or emergencies (snowstorms, earthquakes, hurricanes, etc.) is an important challenge. In this study, a prototype of a self-powered fan based on a thermoelectric system was built to enhance the heat dissipation of the thermoelectric generator (TEG) systems using household stoves as heat sources. To improve output performance of the system, a heat collector consisting of a heat-conducting flat plate and a heat sink with fan cooling was designed to integrate several thermoelectric modules (TEM). The effects of the fan operating conditions (airflow velocity), number of thermoelectric modules, electrical connection mode under different heat flux among the performance of the TEG system are studied. The data obtained showed a higher heat flux and lower flow velocity are required to realize self-sustained cooling of the system. The maximum electric power is more sensitive to the heat flux than the fan operation conditions. It is also observed that more modules provide a higher power output but lower efficiency. The maximum power of four modules in series is larger than that in parallel, and the difference between them increases with increasing heat flux of the heat collector. In the case of self-sufficiency: the maximum output power and maximum net power with four thermoelectric modules are 10.92 W and 5.26 W, respectively, at a heat flux of 30,000 W/m$^2$. Additionally, the maximum conversion efficiency of 1.8% is achieved for two modules at a heat flux of 14,000 W/m$^2$, providing an effective strategy for the installation of TEMs and cooling fans in TEG.

**Keywords:** thermoelectric; fan-cooling; self-powered; heat flux; efficiency

check for updates

**Citation:** Gao, H.; Liu, X.; Zhang, C.; Ma, Y.; Li, H.; Huang, G. Design and Experimental Investigation of a Self-Powered Fan Based on a Thermoelectric System. *Energies* **2023**, *16*, 975. https://doi.org/10.3390/en16020975

Academic Editor: Andrea De Pascale

Received: 3 December 2022
Revised: 29 December 2022
Accepted: 5 January 2023
Published: 15 January 2023

**Copyright:** © 2023 by the authors. Licensee MDPI, Basel, Switzerland. This article is an open access article distributed under the terms and conditions of the Creative Commons Attribution (CC BY) license (https://creativecommons.org/licenses/by/4.0/).

## 1. Introduction

Providing electricity and heating for isolated areas or emergencies (e.g., snowstorms, earthquakes, hurricanes) is an important challenge. A thermoelectric generator (TEG) is an intelligent device that can directly convert heat into electricity via the Seebeck effect of a semiconductor. It has the advantages of no medium leakage, small size, simple structure, and noiseless operation. The stove powered thermoelectric generator could collect wasted heat from a heating stove and convert it into electricity, which will provide both electricity and heating for the residents in remote areas. The power output could be improved by increasing temperature difference between the two ends of the thermoelectric module. A better cooling method is very useful for higher temperature difference. Gao et al. [1] reviewed stove-powered TEGs, and proposed a typical cooling system for a TEG, namely, a water-based natural cooling system, water convection cooling system, air natural cooling system, and air convection cooling system.

In a water-based natural cooling system, a larger water reservoir is usually proposed for stove-powered TEGs as cold side exchangers because of the temperature (maximum 100 °C). For example, Champier et al. [2] built a biomass stove-based TEG with a water tank as the heat sink and an aluminum heat sink as the heat collector, and a maximum electric power of 7.6 W was achieved. Goudarzi et al. [3] obtained approximately 7.9 W power at a matched load from a stove-powered TEG using an aluminum water channel.

Juanicó et al. [4] obtained a maximum electric power of 16 W from an uncontrolled firewood household stove, using a water reservoir as the radiator. In order to prevent the temperature on the cold side of the TEG exceeding 100 °C, a radiator with fan cooling is required to dissipate the heat into the environment. Patowary et al. [5] conducted studies on TEG mounted on modified clay stoves, and tests showed that it was possible to generate 2.7 W of electricity and illuminate a 3 W LED bulb.

As opposed to water reservoir cooling methods, water-forced convection cooling systems usually use pumps and heat sinks as cooling blocks, which have a lower thermal resistance and larger power output than pot cooling systems. Alptekin et al. [6] designed and tested a natural gas-fired boiler-powered TEG using Bi2Te3-based thermoelectric modules. Approximately 36 W power was generated from the TEG unit with cooling water, which was equivalent to one-third of the requirement of the boiler. Montecucco et al. [7] designed a solid-fuel stove-powered TEG with a water-cooled convection system. Hot water was then used for household use or heating. It produced an average power of 600 W with an efficiency of 5%. Sornek et al. [8] examined three types of TEGs, which were mounted on a flue gas channel or flat surface of a wood-fired stove and cooled by air and water convection, respectively. Obernberger et al. [9] developed a wood pellet stove-powered TEG cooled by a water circuit, which produced 50 Wh of electric power to cover its own electricity consumption. Lv et al. [10] designed and analyzed a compact water-cooled thermoelectric generator based on portable gas stove, and a maximum electric power of 12.9 W was obtained. Li et al. [11–13] designed and tested water-cooled, stove-powered TEGs with U-shaped, Ω-shaped, and multiple-notch grooves copper plates as heat collectors. Corresponding electric power outputs of 12.9 W, 62.6 W, 25.7 W, and 200 W were achieved. Zhang et al. [14] set a water-cooled energy exchange short-circuit in TEG to reduce thermal energy loss at the cold side, the results showed that the power is 41.96 mW and the energy conversion efficiency is 1.16%. Tanpradit [15] installed TEG system on liquefied petroleum gas cookstove to utilize waste heat source and adopted circulating water -cooling system for heat dissipation. The power of 107 W was obtained at the average maximum temperature difference of 278.5 °C.

Compared with a water-cooling system, the natural convection of an air system is driven by the buoyant forces of air owing to density change, which has a higher thermal resistance with no moving parts. Nuwayhid et al. [16] obtained a maximum power of 4.2 W with a single TEG module mounted on a woodstove and through natural air convection with higher extended dissipation. Lertsatitthanakorn [17] created a TEG system on a biomass cook stove and obtained approximately 2.4 W power, which was cooled by natural air convection with a rectangular fin heat sink. Yousef et al. [18] built TEGs on a multipurpose stove and natural air convection with larger extrusion heat sinks, and a maximum power of 7.88 W was achieved.

Air convection cooling for TEGs has a fairly low thermal resistance owing to cold cooling by fan cooling. Bass and Killander [19] obtained up to 10 W power from a firewood stove-powered TEG that cooled forced air over a heat sink using a 2 W fan. O'Shaughnessy et al. [20] obtained a maximum power of 5.9 W with a single thermoelectric module, which used portable biomass cook-stoves as the heat source and was cooled by a commercially available heat pipe heat sink and fan. Li and coworkers [21,22] designed a stove-powered TEG using two quarter circle copper plates and two copper flat plates as heat collectors, respectively, and the corresponding maximum electricity power was 8.25 W and 12.9 W with fan cooling. Li et al. [23] further obtained a maximum power of 20.5 W from a gas-fuel combustion-powered TEG with forced convection cooling. Murcinkova et al. [24] tested a stove-powered TEG with air natural and convection cooling, and the corresponding power outputs of 0.5 W and 1.5 W were achieved at a temperature difference of 63 °C and 94 °C, respectively. Martinez et al. [25,26] designed a thermoelectric self-cooling system and reported that the relative thermal resistance between the heat source and ambient air was reduced by 25–30% due to the extended dissipater and fan cooling. Mohammadnia et al. [27] studied the influence of fan operating conditions on the performance of a self-

cooling TEG, and indicated that a minimum inlet airflow external load resistance and temperature were needed for greater net power output.

Although various stove-powered TEGs have been illustrated, only a few studies have been conducted on the enhancement of heat dissipation across the heat collector surface to improve performance of the system. A stove-powered thermoelectric generator with a heat sink and fan cooling was designed to obtain more electricity and deliver more heat from a stove for household heating. For the convenience of testing, the experiment was conducted using an electric heater instead of household stove. The effects of the fan operating conditions (airflow velocity), number of thermoelectric modules, and electrical connection mode under different heat flux among the temperature difference on the power output and efficiency was analyzed.

## 2. Experimental Section

### *2.1. Experimental Setup*

The experimental setup is consisted of an electric heater, a TEG assembly system, an electronic load, and a data acquisition system, as shown in Figure 1. The maximum power of the electric heater was 1500 Watt, which was regulated by a voltage adjuster. The electric heater was an aluminum plate with a diameter of 180 mm and a thickness of 10 mm, around which an aerogel of thickness 30 mm was used as an insulation. The TEG assembly is comprised of a heat collector, thermoelectric modules, and heat sink with fan cooling, where thermoelectric modules are sandwiched between the heat collector and heat sink. The prototype of TEG system was shown in Figure 2. The TEG system contained a heat conducting substrate, thermoelectric modules, fan unit, top shroud, thermocouples, and a hot-wire anemometer. The thermoelectric generator is cooled by 28 fins with a shell of 260 mm in diameter and170 mm in height. Several commercial $Bi_2Te_3$-based thermoelectric modules (Thermonamic: TEP1-12656-0.8) were applied to the TEG, which were clamped between the hot plate and the radiator cooled by a fan. The specific parameters of the thermoelectric module are listed in Table 1.

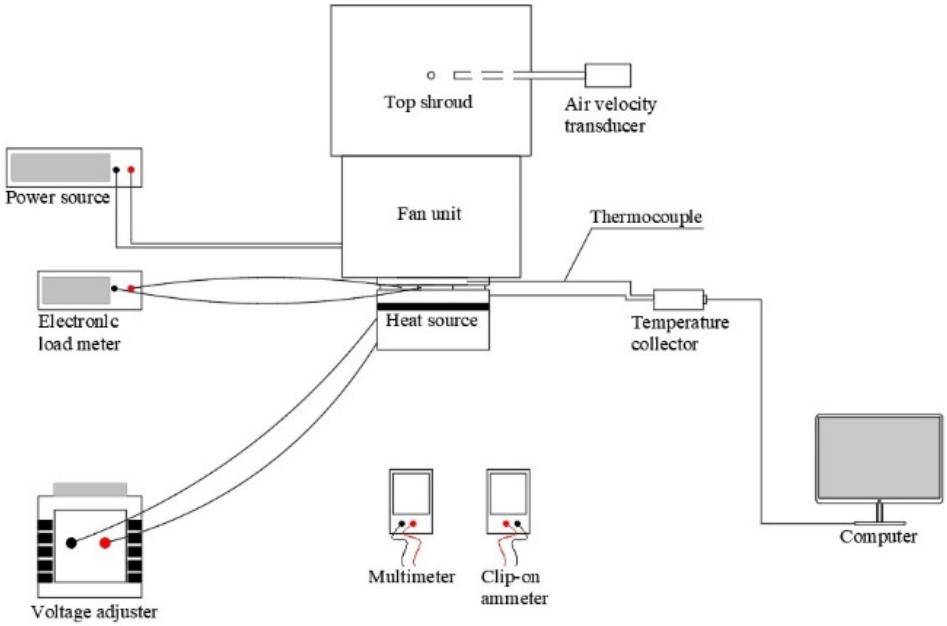



**Figure 1.** Schematic of the experimental setup.

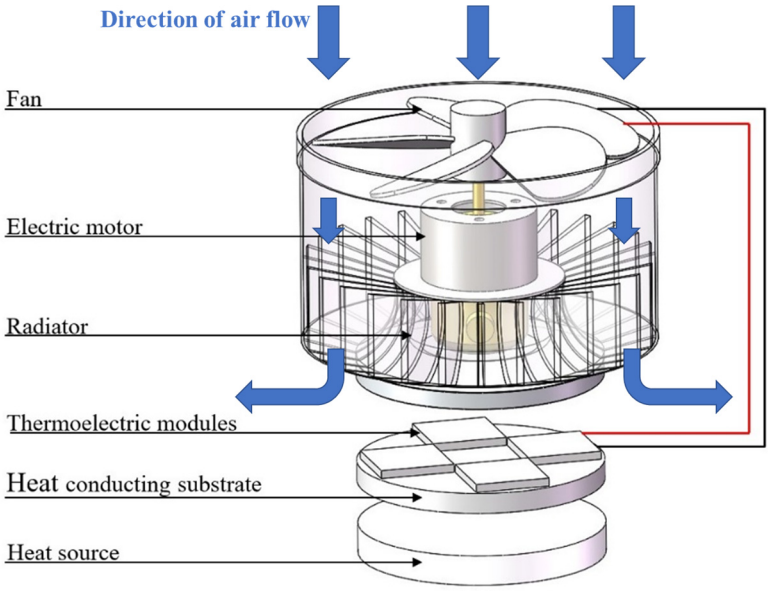



**Figure 2.** Prototype of thermoelectric self-cooling system.

**Table 1.** Specific parameters of thermoelectric module.

| Type | Length (mm) |
|---|---|
| Hot end temperature $T_h$ | 300 °C |
| Cold end temperature $T_c$ | 20 °C |
| Module size | 56 mm × 56 mm × 4 mm |
| Internal resistance | 2.0 Ω |
| Open-circuit voltage (OCV) | 5.0 V |
| Output power | 14.5 W |
| Thermoelectric efficiency | 2.9% |

The airflow test refers to a fan unit installed in the setup shown in Figure 1. The experimental setup of the airflow consisted of a power source, fan unit, top shroud, and a hot-wire anemometer. The shroud was 355 mm high, with an internal diameter (D) equal to the outer diameter of the fan, and was placed on top of the fan. Two holes of diameters 6 mm and 90° apart were located 175 mm from the top of the shroud. The hot-wire anemometer contained a 6 mm diameter probe of sufficient length to insert into the center of the shroud. The air flows down from the top of heat radiator under the drive of the fan, as shown in Figure 2. The air at the top of house could be further heated, which can reduce the vertical temperature gradient in the heating space through forced convection, making the indoor temperature relatively uniform.

Before the test starts, the power input of the electric hot plate was adjusted to a set heat flux, and the fan unit operation was allowed to stabilize until the base temperature remained constant. The air velocity and flow rate produced by the fan were measured and calculated as follows. The inner areas of the shroud were divided into five equal areas, as shown in Figure 3. The air velocity of each area was measured by inserting a hot-wire anemometer probe through the holes located in the middle of each area inside the shroud. Measurement points are shown from points 1 to 5 in Figure 3. The probe tip was inserted into the other hole and the aforementioned operation was repeated for each of the five points listed in Table 2. The average air velocity of the fan was considered as the average of each velocity on five points owing to the equal areas of five zones. The fan power input was adjusted for various air velocities and the entire procedure was repeated for different heat fluxes.

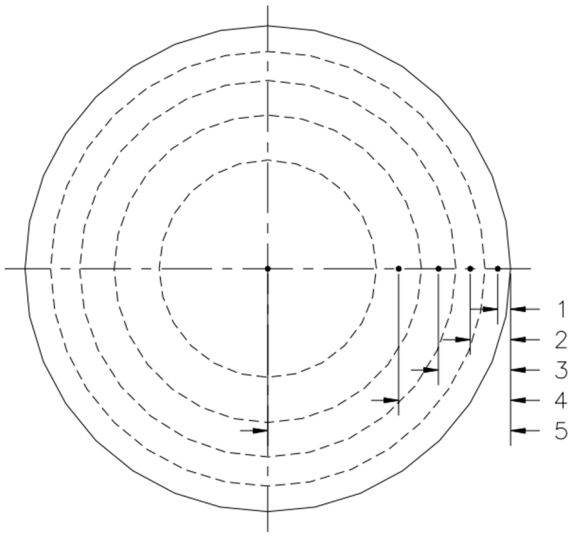



**Figure 3.** Flow velocity measurement points.

**Table 2.** Insertion length of air velocity transducer.

| Point | Length (mm) |
|---|---|
| 1 | 0.053 × D/2 |
| 2 | 0.166 × D/2 |
| 3 | 0.297 × D/2 |
| 4 | 0.461 × D/2 |
| 5 | 1.000 × D/2 |

The output voltage and power were obtained using the electronic load as the external load, and the voltage and current of the heaters and fans were obtained using millimeters and clip-on meters. Two T-type thermocouples were mounted on the heat collection plate and heat sink to measure the temperatures of both thermoelectric sides. Temperature signals were collected and recorded using an acquisition system (Agilent 34972A). The uncertainties of the temperature, heating power, heat flux, power output, conversion efficiency, and flow velocity were obtained using the root-sum-squares (RSS) method [28], which are listed in Table 3.

**Table 3.** Uncertainty for measured variable.

| Variable | Uncertainty | Variable | Uncertainty |
|---|---|---|---|
| $T_h$ | 3.1% | $T_c$ | 3.5% |
| $P_{TE}$ | 2.6% | $Q_H$ | 2.9% |
| $\eta_{TE}$ | 3.3% | $q$ | 3.6% |
| $v_{fan}$ | 4.1% | | |

### *2.2. Experimental Procedure and Parameter Definitions*

The power of the electric heater was adjusted by a voltage adjuster. The heat flux through the TEG is obtained from the power of the electric heater and the surface area across the heater. The current and voltage were measured using a clip-on meter and a millimeter, and the corresponding heat flux across the TEG was obtained using Equation (1).

$$q = \frac{Q_H}{A} = \frac{U_H I_H}{A} \tag{1}$$

where $q$ and $A$ are the heat flux and surface area across the heater, $Q_H$, $U_H$, and $I_H$ are the electric power input, voltage, and current of the electric heating plate, respectively.

The air flow velocity was also adjusted to the desired value by changing the power of the fan. The related air flow velocity was measured and accurately calculated using an air hot-wire anemometer. The power output of the fan was acquired by measuring the voltage and current, as shown in Equation (2).

$$P_{fan} = U_{fan} I_{fan} \tag{2}$$

where $P_{fan}$, $U_{fan}$, and $I_{fan}$ are the power, voltage, and current of the fan, respectively.

The system is considered stable when the cold and hot-side temperatures basically remain unchanged within 10 min. The temperatures of both sides of the TEG were measured and recorded using an Agilent 34972A acquisition system. The voltage and current of the TEG were measured by adjusting the electrical load, and the corresponding maximum output power and thermoelectric efficiency were obtained from Equations (3) and (4), respectively.

$$P_{TE} = U_{TE} I_{TE} \tag{3}$$

$$\eta_{TE} = \frac{P_{TE}}{Q_H} \tag{4}$$

where $P_{TE}$, $U_{TE}$, $I_{TE}$, and $\eta_{TE}$ are the power output, voltage, current, and thermoelectric efficiency of the TEG, respectively.

## 3. Results and Discussion

As mentioned earlier, various air flow velocities and heat fluxes were acquired by adjusting the electrical power, which affected the hot and cold-side temperatures of the TEG and the corresponding temperature difference between them, thermoelectric modules are in series as shown in Figure 4. It is observed that the hot and cold-side temperatures of the TEG slightly decline, while the corresponding temperature differences are almost unchanged with increasing flow velocity for a fixed heat flux. For example, the temperature of the TEG on both hot and cold sides is reduced from 79.4 °C to 60.7 °C and 44.5 °C to 27.4 °C, respectively, and the corresponding temperature difference is changed from 34.9 °C to 32.3 °C as the air flow velocity increases from 0.30 m/s to 1.3 m/s for a given heat flux of 6000 W/m$^2$. This is because the convective heat transfer coefficient at the cold side of the TEG is increased with the increase in flow velocity, leading to a lower thermal resistance at the cold side and lower average temperature of the TEG. Furthermore, the thermal conductivity of the TEG first declines and then increases with increasing temperature of the TEG, as shown in reference [29]. There is a tiny decline for the thermal conductivity with the decrease of TEG temperature at the present case. For a fixed heat flux, the thermal resistance is proportional to the temperature difference. Thus, the temperature difference across the thermoelectric module is almost unchanged with the increase of flow velocity, whereas the hot and cold side temperature of thermoelectric module is declined.

Moreover, the temperature of the TEG on the hot side is significantly increased, whereas the temperatures on the cold side ascend mildly with increasing heat flux for various flow velocities. The corresponding temperature difference across the TEG is also amplified, and the tendency weakens with increasing heat flux. This is because the thermal resistance of the heat collector and cold heat sink remain nearly constant, while the thermal resistance of the thermoelectric modules decreases with increase in the temperature of the TEG due to increase in thermal conductivity. For example, the temperatures of the TEG on the hot and cold sides are increased from 65.7 °C to 246.0 °C and 30.8 °C to 86.3 °C, respectively, and the corresponding temperature difference is increased from 34.9 °C to 159.7 °C as the heat flux increases from 6000 W/m$^2$ to 30,000 W/m$^2$ at a velocity of 0.80 m/s. This indicates that the heat flux across the heat collector has a dramatic effect on the hot-side temperature and the corresponding temperature difference across the TEG, which has a minor effect on the cold-side temperature of the TEG for a given flow velocity.

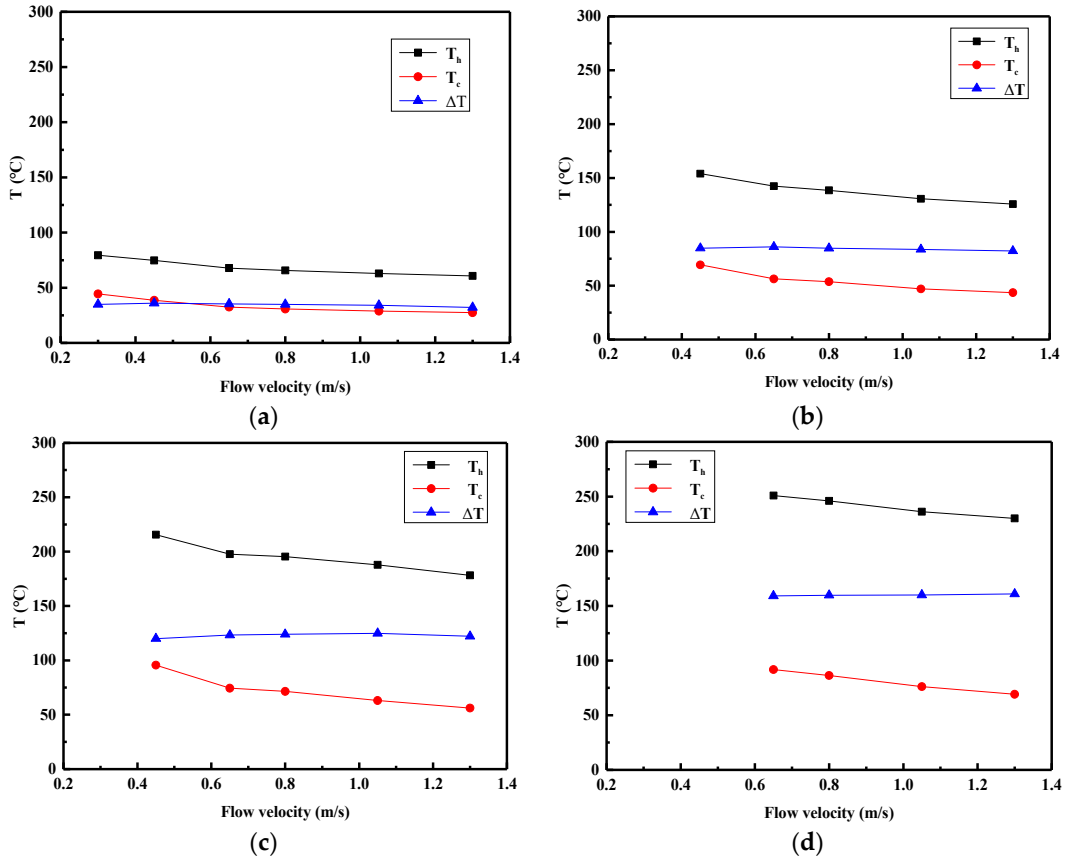



**Figure 4.** (**a**) 6000 W/m$^2$, (**b**) 14,000 W/m$^2$, (**c**) 22,000 W/m$^2$, (**d**) 30,000 W/m$^2$. Temperatures at various air flow velocity and heat flux with four thermoelectric modules.

To further illustrate this, the temperature profile from the hot plate to ambient air is shown in Figure 5. The thermal resistance of the cold heat sink decreases with increasing air flow velocity, leading to a lower cold-side temperature and a resultant higher temperature difference for a given heat flux (from dashed line b to solid line a). Moreover, the temperature difference is significantly decreased owing to the reduction in the hot-side temperature and heat flux through the heat collector (from solid line a to dotted line c).

The maximum power output at various air flow velocities and heat fluxes is displayed in Figure 6, and the corresponding consumption power of the fan is used as a reference. The maximum power output is acquired as in reference [30] when the internal load of the TEG matches the external load. Generally, the power output is approximately the square of the temperature difference between the two ends of the thermoelectric module. Hence, the power output evidently increases with increase in heat flux owing to increasing temperature difference through the TEG, as shown in Figure 4. Moreover, the power output is slightly increased and then declines with increase in the air flow velocity or thermoelectric module number for a given heat flux. The peak power is generated at the heat flux of 6000 W/m$^2$ when the flow velocity is 0.45 m/s, and at the heat flux of 10,000 W/m$^2$ and 14,000 W/m$^2$ when the flow velocity is 0.80 m/s for one module and two modules, respectively. Furthermore, the maximum power is generated at a heat flux of 18,000 W/m$^2$ when the flow velocity is 1.05 m/s for two modules. Similarly, the peak power output is generated at the heat flux of 6000 W/m$^2$ and 10,000 W/m$^2$ when the flow velocity is 0.45 m/s, and at the heat flux of 14,000 W/m$^2$ when the flow velocity is 0.65 m/s for three modules. When the flow velocity is 1.05 m/s for three modules and four modules, the peak power is generated at the heat flux of 18,000 W/m2 and 26,000 W/m$^2$, respectively. However, although the maximum power output of the TEG increases with increase in the thermoelectric module number, the maximum power output for each thermoelectric

module declines with increase in the thermoelectric module number within the allowable temperature. For example, the total power output of the TEG increases from 5.8 W to 11.4 W, while the power output of each thermoelectric module is reduced from 5.8 W to 2.85 W with increasing number of thermoelectric modules within the allowable temperature. The self-sufficient operation can be achieved by adjusting the air flow velocity at different heat flux. In the case of self-powered conditions, the maximum output power of TEG is 10.92 W, and the maximum net power is 5.26 W.

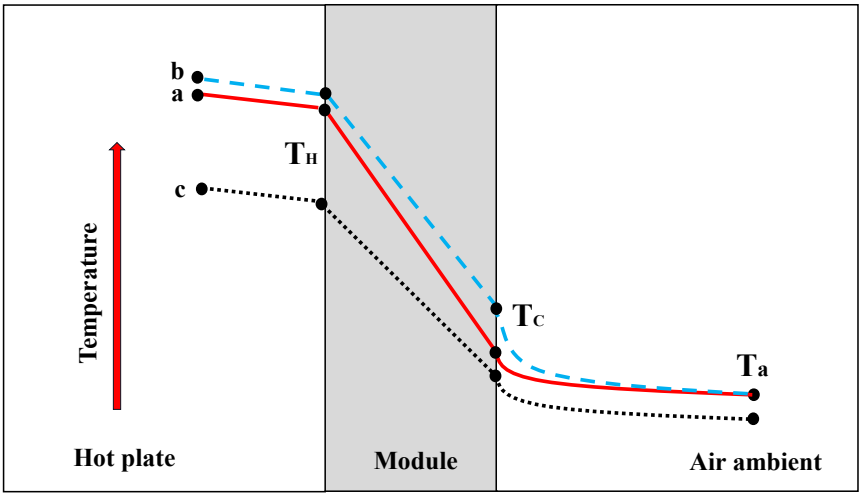



**Figure 5.** Temperature Profiles from hot plate to air ambient. (a) Aluminum hot plate and heat sink with fan cooling. (b) As in (a), but with a lower flow velocity. (c) As in (a), but with a lower heat flux.

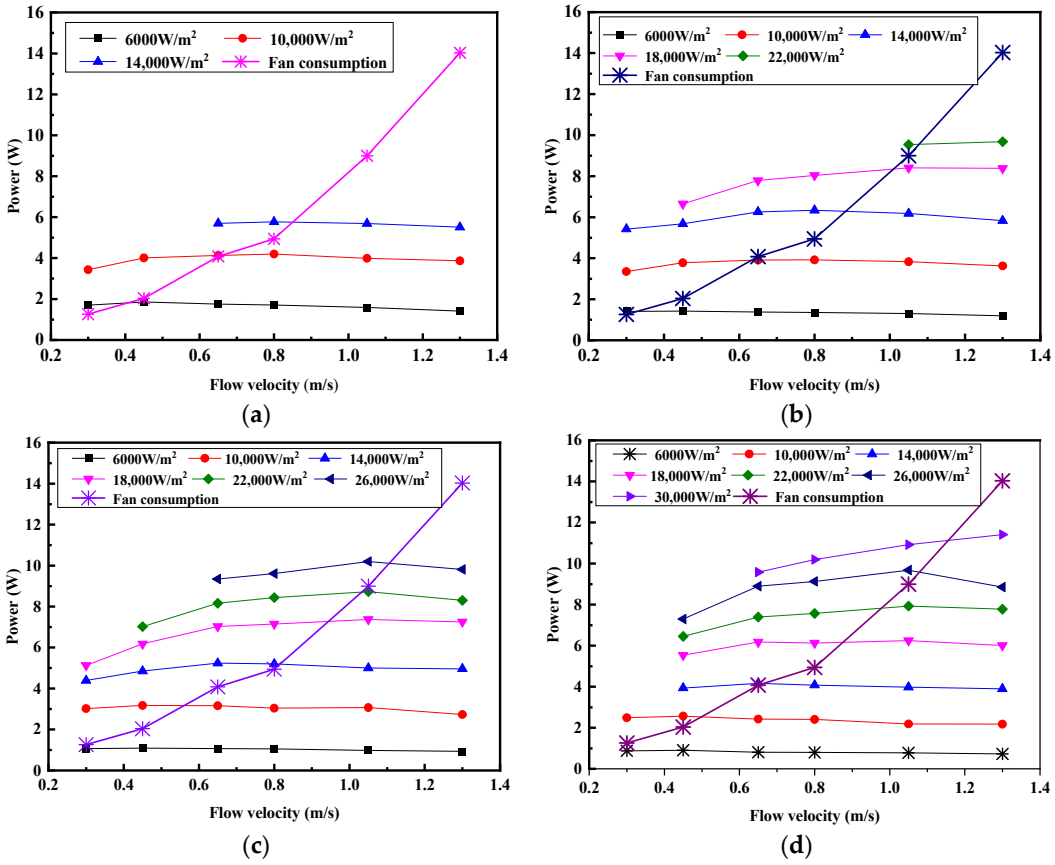



**Figure 6.** (**a**) one module, (**b**) two modules, (**c**) three modules, (**d**) four modules. Maximum power output at various air flow velocity and heat flux.

The thermoelectric efficiency is shown in Figure 7, which can be obtained from the power input of the heat source and power output, as shown in Equation (4). The efficiency increases slightly and then decreases with increasing flow velocity at a fixed heat flux. This is because the temperature difference of the TEG is slightly increased, while the thermal conductivity and hot side temperature weakly decline with increase in flow velocity, as shown in Figure 5. As shown by Rowe et al. [30], the conversion efficiency is positively associated with the temperature difference and the figure of merit Z of the TEG, and is negatively associated with the thermal conductivity and hot side temperature of the TEG. Similarly, the conversion efficiency first increases and then decreases with increase in the heat flux of the heat collector. This is because the hot side temperature, temperature difference across the TEG, and the thermal conductivity all increase with increasing heat flux. Furthermore, the conversion efficiency decreases continuously with increasing number of modules for a given heat flux and flow velocity. This is because there is a higher temperature on the hot side and larger temperature difference between the double sides of the TEG with fewer thermoelectric modules owing to the increasing heat flux of each module. The thermal resistance on the cold side declines with decrease in the number of modules owing to the larger heat dissipation area for each module. Under the competition of the temperature difference, hot-side temperature, and thermal resistance on the cold side, a maximum conversion efficiency of 1.8% is achieved for the two modules at a heat flux of 14,000 W/m$^2$ under self-powered conditions as shown in Figure 7b.

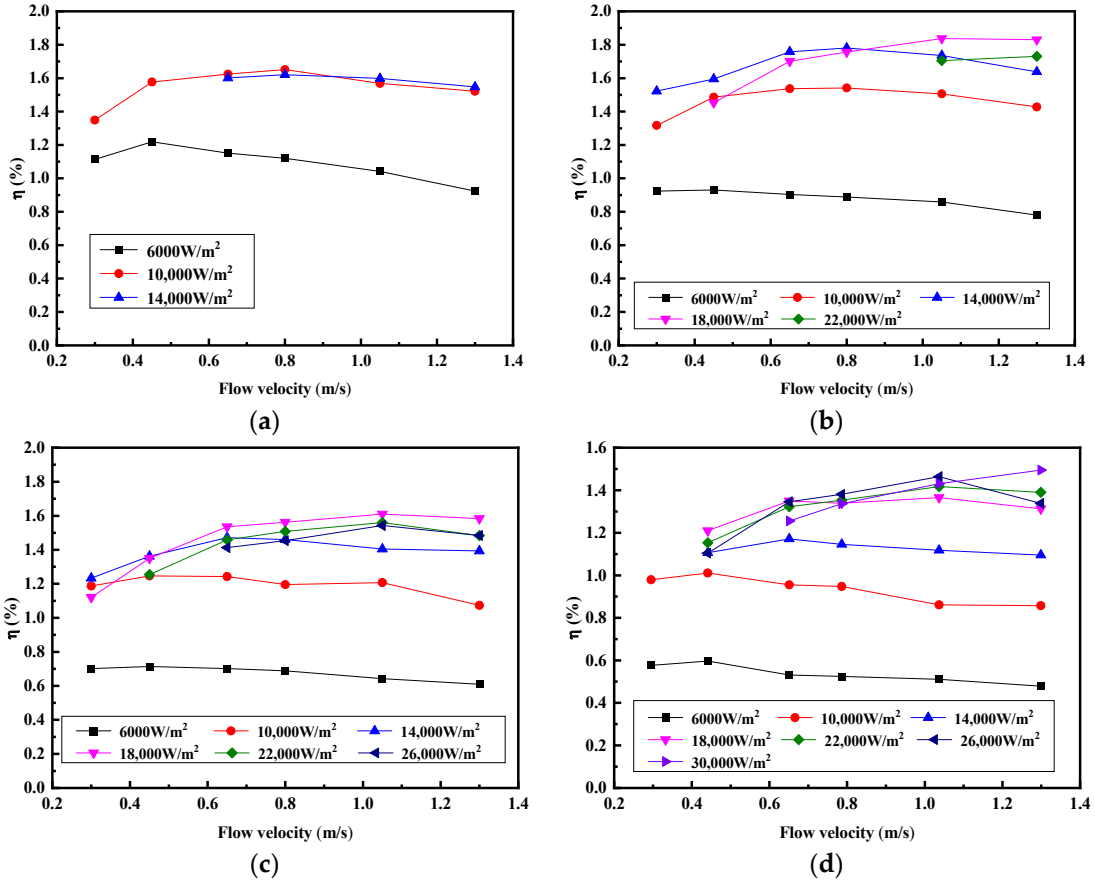



**Figure 7.** (**a**) one module, (**b**) two modules, (**c**) three modules, (**d**) four modules. Thermoelectric efficiency at various air flow velocity and heat flux.

The connection mode of the thermoelectric modules also influences the thermoelectric performance, and the effect of the connection mode on the power output of the four modules is shown in Figure 8 at a fixed flow velocity of 1.037 m/s. Generally, the maximum

power of four modules in series is greater than that in parallel. The difference between series and parallel configurations increases with increasing heat flux of the heat collector. The corresponding connections of the four modules in series and parallel are shown in Figure 9, where each module is represented by the voltage sources V1, V2, V3, and V4, respectively. The reason for the power loss is the additional wire and connectors. However, the performances in series and parallels are almost the same because of the identical number of connections for ideal conditions. Several junctions exist in the parallel circuits. The existence of a junction implies that the current can propagate through multiple pathways in the circuit. The current mainly travels along a path with low resistance when it reaches the intersection. Therefore, the power output decreases with increase in the junction number in the array configuration circuit. The power loss depends on the proportion of the current in the circuit. However, the temperature difference is different for each module in a practical system due to the different heat fluxes across the modules, resulting in different power outputs and electrical resistances for each module. Therefore, the difference in performance in series and parallel configurations increases with increasing heat flux owing to the number of connections and unbalanced power output.

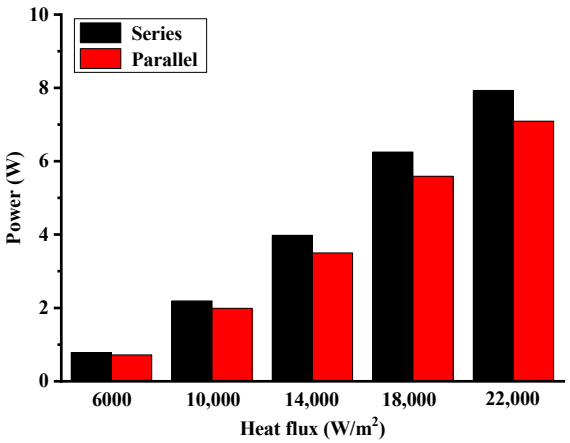



**Figure 8.** Comparison of connection mode on power output with four thermoelectric modules.

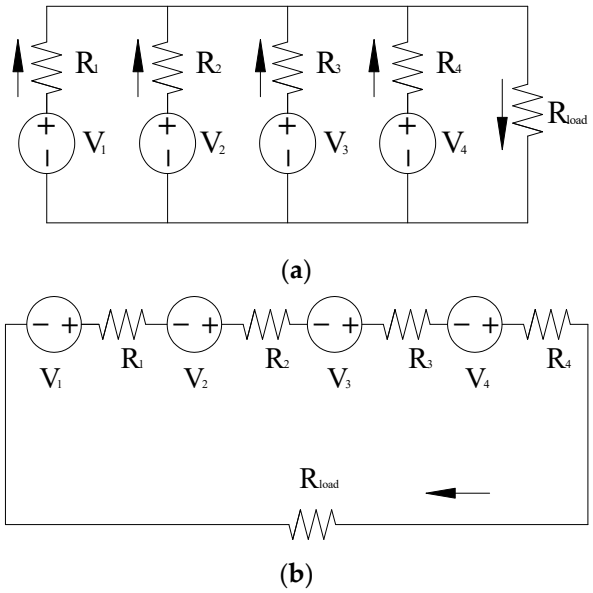



**Figure 9.** (**a**) parallel, (**b**) series. Electrical schematic of an array of four TEG modules electrically connected in parallel and series.

## 4. Conclusions

A self-powered fan was designed, and the effects of the flow velocity, heat flux through the heat collector, module number, and electrical connection mode on the performance of the TEG were investigated. For a given number of modules, the temperature difference across the TEG remains almost unchanged with variation in the flow velocity at a fixed heat flux. The heat flux through the heat collector has a dramatic effect on the hot-side temperature and the temperature difference across the TEG, which has a minor effect on the cold-side temperature of the TEG. Consequently, the power output is more sensitive to the heat flux and is less dependent on the flow velocity. The power output evidently increases with increase in heat flux, and slightly increases and then declines with increase in the air flow velocity or thermoelectric module number for a given heat flux. The maximum output power of the TEG is increased from 5.8 W to 11.4 W, while the power output of each thermoelectric module is reduced from 5.8 W to 2.85 W when the number of modules is increased from one to four within the allowable temperature of the thermoelectric module. In the case of self-powered conditions, the maximum output power of TEG is 10.92 W, and the maximum net power is 5.26 W. The conversion efficiency is slightly increased and then decreases with an increase in flow velocity or heat flux when other conditions remain constant, and a maximum conversion efficiency of 1.8% is achieved for the two modules at a heat flux of 14,000 $W/m^2$. The maximum power of four modules in series is higher than that in parallel. The difference between series and parallel configurations increases with increasing heat flux of the heat collector. The heat source conditions of this experiment are relatively stable. Considering the temperature fluctuation during the combustion of household stoves, the subsequent experiments should be carried out on specific household stoves for verification. The opposite air flow direction will study with another fan in counter rotation and compare with the present case in the future work. For the TEG system with domestic stoves as the heat source, setting the appropriate flow velocity of fan for different surface temperature will result in better output performance. More heat is delivered from the stove to the environment due to the forced convection with the self-powered fan compared with the natural convection without the cooling of the fan. The thermal efficiency of the stove will also be conducted in the future work.

**Author Contributions:** All the authors made contributions to the concept and design of the article. Conceptualization, H.G.; Methodology, H.G. and C.Z.; Software, H.G. and X.L.; Validation, H.G. and Y.M.; Formal Analysis, H.G. and H.L.; Investigation, H.G. and G.H.; Resources, H.G.; Data Curation, H.G.; Writing—Original Draft Preparation, H.G.; Writing—Review & Editing, H.G.; Visualization, H.G.; Supervision, H.G. All authors have read and agreed to the published version of the manuscript.

**Funding:** This work was supported by the Natural Science Foundation of China (52176132), Natural Science Foundation of Shaanxi Province of China (2018JM5077) and Innovative talents cultivate program of Shaanxi (2021TD-27).

**Data Availability Statement:** The data presented in this study are available in this article.

**Conflicts of Interest:** The authors declare no conflict of interest.

## References

1. Gao, H.B.; Huang, G.H.; Li, H.J.; Qu, Z.G.; Zhang, Y.J. Development of stove-powered thermoelectric generators: A review. *Appl. Therm. Eng.* **2016**, *96*, 297–310. [CrossRef]
2. Champier, D.; Bedecarrats, J.P.; Kousksou, T.; Rivaletto, M.; Strub, F.; Pignolet, P. Study of a TE (thermoelectric) generator incorporated in a multifunction wood stove. *Energy* **2011**, *36*, 1518–1526. [CrossRef]
3. Goudarzi, A.M.; Mazandarani, P.; Panahi, R.; Behsaz, H.; Renania, A.; Rosendahl, L.A. Integration of thermoelectric generators and wood stove to produce heat, hot water, and electrical power. *J. Electron. Mater.* **2013**, *42*, 2127–2133. [CrossRef]
4. Juanicó, L.E.; Rinalde, F.; Taglialavore, E.; Molina, M. Novel heat controller for thermogenerators working on uncontrolled stoves. *J. Electron. Mater.* **2013**, *42*, 1776–1780. [CrossRef]
5. Patowary, R.; Baruah, D.C. Feasibility study of TEG-integrated biomass cook stove for electrical power generation specific to rural areas with inadequate electricity. *Energy Sources Part A Recovery Util. Environ. Eff.* **2019**, 1–22. [CrossRef]

6. Alptekin, M.; Calisir, T.; Baskaya, S. Design and experimental investigation of a thermoelectric self-powered heating system. *Energy Convers. Manag.* **2017**, *146*, 244–252. [CrossRef]
7. Montecucco, A.; Siviter, J.; Knox, A.R. Combined heat and power system for stoves with thermoelectric generators. *Appl. Energy* **2017**, *185*, 1336–1342. [CrossRef]
8. Sornek, K.; Filipowicz, M.; Żołądek, M.; Kot, R.; Mikrut, M. Comparative analysis of selected thermoelectric generators operating with wood-fired stove. *Energy* **2019**, *166*, 1303–1313. [CrossRef]
9. Obernberger, I.; Weiß, G.; Kössl, M. Development of a new micro CHP pellet stove technology. *Biomass Bioenergy* **2018**, *116*, 198–204. [CrossRef]
10. Lv, H.K.; Li, G.N.; Zheng, Y.Q.; Hu, J.G.; Li, J. Compact water-cooled thermoelectric generator (TEG) based on a portable gas stove. *Energies* **2018**, *11*, 2231. [CrossRef]
11. Li, G.N.; Zheng, Y.Q.; Hu, J.G.; Guo, W.W. Experiments and a simplified theoretical model for a water-cooled, stove-powered thermoelectric generator. *Energy* **2019**, *185*, 437–448. [CrossRef]
12. Li, G.N.; Zhu, D.Y.; Zheng, Y.Q.; Guo, W.W. Mesoscale combustor-powered thermoelectric generator with enhanced heat collection. *Energy Convers. Manag.* **2020**, *205*, 112403. [CrossRef]
13. Li, G.N.; Zheng, Y.Q.; Lv, H.K.; Hu, J.G.; Li, J.; Guo, W.W. Micro combined heat and power system based on stove-powered thermoelectric generator. *Renew Energy* **2020**, *155*, 160–171.
14. Zhang, Z.; Zhang, Y.Q.; Sui, X.M.; Li, W.B.; Xu, D.C. Performance of thermoelectric power-generation system for sufficient recovery and reuse of heat accumulated at cold side of TEG with water-cooling energy exchange circuit. *Energies* **2020**, *13*, 5542. [CrossRef]
15. Tanpradit, D. The development of waste heat energy conversion device to generate electricity through thermoelectric generator (TEG) apply to LPG cookstove. *RMUTP Res. J.* **2020**, *14*, 193–207.
16. Nuwayhid, R.Y.; Shihadeh, A.; Ghaddar, N. Development and testing of a domestic woodstove thermoelectric generator with natural convection cooling. *Energy Convers. Manag.* **2005**, *46*, 1631–1643. [CrossRef]
17. Lertsatitthanakorn, C. Electrical performance analysis and economic evaluation of combined biomass cook stove thermoelectric (BITE) generator. *Bioresour. Technol.* **2007**, *98*, 1670–1674. [CrossRef]
18. Najjar, Y.S.H.; Kseibi, M.M. Heat transfer and performance analysis of thermoelectric stoves. *Appl. Therm. Eng.* **2016**, *102*, 1045–1048. [CrossRef]
19. Killander, A.; Bass, J.C. A stove-top generator for cold areas. In Proceedings of the Fifteenth International Conference on Thermoelectrics, Pasadena, CA, USA, 26–29 March 1996; IEEE: Piscataway, NJ, USA, 1996; pp. 390–393.
20. O'Shaughnessy, S.M.; Deasy, M.J.; Kinsella, C.E.; Doyle, J.V.; Robinson, A.J. Small scale electricity generation from a portable biomass cookstove: Prototype design and preliminary results. *Appl. Energy* **2013**, *102*, 374–385. [CrossRef]
21. Zheng, Y.; Hu, J.; Li, G.; Zhu, L.; Guo, W. Testing and optimizing a stove-powered thermoelectric generator with fan cooling. *Materials* **2018**, *11*, 966. [CrossRef]
22. Li, G.N.; Zhang, S.; Zheng, Y.; Zhu, L.; Guo, W. Experimental study on a stove-powered thermoelectric generator (STEG) with self starting fan cooling. *Renew Energy* **2018**, *121*, 502–512. [CrossRef]
23. Li, G.N.; Yi, M.B.; Tulu, M.B.; Zheng, Y.Q.; Guo, W.W.; Tang, Y.J. Miniature self-powering and self-aspirating combustion-powered thermoelectric generator burning gas fuels for combined heat and power supply. *J. Power. Sources* **2021**, *506*, 230263. [CrossRef]
24. Murčinková, Z.; Kosturák, M.; Ferenc, J. Testing of proposed design of stove-powered thermoelectric generator using natural and forced air cooling. *Adv. Mech. Eng.* **2021**, *13*, 1–10. [CrossRef]
25. Martinez, A.; Astrain, D.; Rodriguez, A. Experimental and analytical study on thermoelectric self cooling of devices. *Energy* **2011**, *36*, 5250–5260. [CrossRef]
26. Martinez, A.; Astrain, D.; Rodriguez, A. Dynamic model for simulation of thermoelectric self cooling applications. *Energy* **2013**, *55*, 1114–1126. [CrossRef]
27. Mohammadnia, A.; Ziapour, B.M.; Sedaghati, F.; Rosendahl, L.; Rezania, A. Fan operating condition effect on performance of self-cooling thermoelectric generator system. *Energy* **2021**, *224*, 120177. [CrossRef]
28. Moffat, R.J. Describing the uncertainties in experimental results. *Exp. Therm. Fluid Sci.* **1988**, *1*, 3–17. [CrossRef]
29. Gao, H.B.; Zong, S.C.; Zhang, C.W.; Li, H.J.; Huang, G.H. Experimental investigation of the performance of a thermoelectric generator at various operating conditions. *IOP Conf. Ser. Earth Environ. Sci.* **2021**, *702*, 012001. [CrossRef]
30. Rowe, D.M.; Gao, M. Evaluation of thermoelectric modules for power generation. *J. Power Sources* **1998**, *73*, 193–198. [CrossRef]


**Disclaimer/Publisher's Note:** The statements, opinions and data contained in all publications are solely those of the individual author(s) and contributor(s) and not of MDPI and/or the editor(s). MDPI and/or the editor(s) disclaim responsibility for any injury to people or property resulting from any ideas, methods, instructions or products referred to in the content.